CrossMark

SIMB
Society for Industrial Microbiology
and Biotechnology

GENETICS AND MOLECULAR BIOLOGY OF INDUSTRIAL ORGANISMS

Growth retardation of *Escherichia coli* by artificial increase of intracellular ATP

Yoon-Ah Na[1] · Joo-Young Lee[1] · Weon-Jeong Bang[1] · Hyo Jung Lee[1] · Su-In Choi[1] ·
Soon-Kyeong Kwon[3] · Kwang-Hwan Jung[2] · Jihyun F. Kim[3] · Pil Kim[1]

Abstract Overexpression of phosphoenolpyruvate carboxykinase (PCK) was reported to cause the harboring of higher intracellular ATP concentration in *Escherichia coli*, accompanied with a slower growth rate. For systematic determination of the relationship between the artificial increase of ATP and growth retardation, PCK_{WT} enzyme was directly evolved in vitro and further overexpressed. The evolved PCK67 showed a 60 % greater catalytic efficiency than that of PCK_{WT}. Consequently, the PCK67-overexpressing *E. coli* showed the highest ATP concentration at the log phase of 1.45 $\mu mol/g_{cell}$, with the slowest growth rate of 0.66 h^{-1}, while the PCK_{WT}-overexpressing cells displayed 1.00 $\mu mol/g_{cell}$ ATP concentration with the growth rate of 0.84 h^{-1} and the control had 0.28 $\mu mol/g_{cell}$ with 1.03 h^{-1}. To find a plausible reason, PCK-overexpressing cells in a steady state during chemostat growth were applied to monitor intracellular reactive oxygen species (ROS). Higher amount of intracellular ROS were observed as the ATP levels increased. To confirm the hypothesis of slower growth rate without perturbation of the carbon flux by PCK-overexpression, phototrophic *Gloeobacter* rhodopsin (GR) was expressed. The GR-expressing strain under illumination harbored 81 % more ATP concentration along with 82 % higher ROS, with a 54 % slower maximum growth rate than the control, while both the GR-expressing strain under dark and dicarboxylate transporter (a control membrane protein)-expressing strain showed a lower ATP and increased ROS, and slower growth rate. Regardless of carbon flux changes, the artificial ATP increase was related to the ROS increase and it was reciprocally correlated to the maximum growth rate. To verify that the accumulated intracellular ROS were responsible for the growth retardation, glutathione was added to the medium to reduce the ROS. As a result, the growth retardation was restored by the addition of 0.1 mM glutathione. Anaerobic culture even enabled the artificial ATP-increased *E. coli* to grow faster than control. Collectively, it was concluded that artificial ATP increases inhibit the growth of *E. coli* due to the overproduction of ROS.

Keywords Phosphoenolpyruvate carboxykinase · High intracellular ATP concentration · Growth retardation · ROS-scavenging

Y.-A. Na, J.-Y. Lee, and W.-J. Bang are authors contributed equally to the work.

✉ Pil Kim
kimp@catholic.ac.kr

[1] Department of Biotechnology, The Catholic University of Korea, Bucheon 420-743, Gyeonggi, Korea

[2] Department of Life Science, Sogang University, Seoul 121-742, Korea

[3] Department of Systems Biology, Yonsei University, Seoul 120-749, Korea

Introduction

In *Escherichia coli*, phosphoenolpyruvate (PEP), a C3 metabolite of the glycolysis, is carboxylated into oxaloacetate (OAA), a C4 metabolite of the TCA cycle, via phosphoenolpyruvate carboxylase (PPC, EC 4.1.1.31) under glycolytic conditions [4, 7]. The OAA is decarboxylated into PEP under gluconeogenic conditions via phosphoenolpyruvate carboxykinase (PCK, EC 4.1.1.49) in vivo [4, 16, 36]. However, examination of the enzymatic characteristics in vitro revealed that PCK could also mediate the reversible reaction under conditions of high CO_2 concentrations, and that the carboxylation of PEP by PCK could

🖄 Springer

result in the production of ATP, as opposed to PPC, which produces inorganic phosphate [4, 5, 21]. The overexpression of PCK enabled *E. coli* to harbor higher ATP concentration [13, 19, 20], which in turn allowed the *E. coli* to achieve enhanced expression and secretion of recombinant protein [12]. It was suggested that the enhanced protein production facilitated by the artificial increase of ATP was due to the up-regulation of genes in biosynthetic pathways, increase of ribosome concentration, and activation of the amino acid-charging reactions on tRNAs. Although the harboring of higher ATP concentration via PCK-overexpression was proven to be beneficial for the production of recombinant protein, the limitation of retarded host's growth rate was also observed. The PCK-overexpressing *E. coli* was reported to have a 20 % decrease in the growth rate [20]. A similar phenomenon was also observed in the *E. coli* strains harboring greater reducing equivalents [14, 15, 18], either through the overexpression of NADH-dependent malic enzyme (MaeA), or in phosphoglucose isomerase (*pgi*)-disrupted *E. coli*. The resulting increases of both [NADH] and [NADPH] resulted in decreased growth rates [14].

The degree of artificial ATP increase by plasmid-derived PCK-overexpression was thought to be altered by modified enzymatic activity [21]. The directed evolution of enzymes has been a powerful technique for the improvement of enzymatic characteristics, such as providing faster turnover rate [11] and modification of the optimal conditions [30]. It has not yet been determined whether the growth retardation of the PCK-overexpressing *E. coli* could be altered by the modification of PCK enzyme activity.

Bacteriorhodopsin is a proton-pumping membrane-integrated protein present in many cyanobacteria [17, 27]. Photon absorption on retinal, a prosthetic molecule in bacteriorhodopsin, triggers isomerization and release of a proton outside the membrane, resulting in the generation of proton motive force. Lee and Jung reported that the expression of a bacteriorhodopsin from *Gloeobacter violaceus* PCC7421, a primitive cyanobacteria, caused regeneration of light-driven ATP in a membrane inverted system of *E. coli* [6, 23, 27]. Expression of the *Gloeobacter* rhodopsin (GR) in *E. coli* was predicted as another way of artificially increasing the ATP concentration without perturbation of the carbon flux.

In this light, we report that the overexpression of a directly evolved PCK, as well as *Gloeobacter* rhodopsin with illumination of the culture, can help to gain an understanding of the relationship between retarded growth rate and the artificial increase of ATP in *E. coli*. Steady-state cells overexpressing PCK$_{WT}$ from chemostat cultures with different dilution rates were also used to verify the relationship. A reason for the retarded growth observed in the *E. coli* with artificial ATP increase is suggested based on the results.

Materials and methods

Strains and plasmids

All strains and plasmids used in this study are listed in Table 1. *E. coli* W3110 (Korean Collection of Type Culture, KCTC 2223) and its derivatives were used for studies on the relationship between artificial ATP increase and growth rate. *E. coli* DH5α (Invitrogen, CA, USA) was utilized for plasmid construction and propagation. *E. coli* ER2566 (NEB, MA, USA) was used for the expression host in the directed evolution of PCK. Standard molecular cloning procedures were utilized herein [34].

The plasmids carrying the genes encoding *E. coli* PCK (pEcPck) and *Gloeobacter* rhodopsin (pKJ606-GR) were described in previous studies [19, 23]. To verify the effect of membrane protein expression as control, the gene of dicarboxylate transporter (*dctA*) from *E. coli* were PCR-amplified based on the pTrc(P$_{lac}$*hemA*$^+$-*maeB-dctA*) template [24] and the oligonucleotides of <u>CATATG</u>AAAACCTC TCTGTTTAAAAGCC (*Nde* I site underlined) and <u>GCG-GCCGC</u>TTAAGAGGATAATTCGT (*Not* I site underlined). The DNA fragments (1.3 kb) were sub-cloned into a T-vector (T-blunt, Solgent Co., Daejeon, Korea). After sequence verification, the T-vectors containing PCR-fragments were double-digested with *Nde* I-*Not* I and the DNA fragment (1.3 kb) were ligated with the 9.0 kb fragment of the same digested pKA001 (the same with the parental vector of pKJ606-GR except a *Nde* I site removal), resulting in pKJ606-*dctA*.

Escherichia coli PEP carboxykinase (*pckA*) was directly evolved by introducing random mutations, followed by screening based on the PEP carboxylation activity, according to the method in a previous study [11]. A random mutation was introduced into the *pckA* gene by an error-prone PCR mutagenesis kit (ClonTech Laboratories, CA, USA) with a mutation rate of 2.7 mutations/kb using the pEcPck plasmid DNA as a PCR template and the following oligonucleotides: 5′-<u>CATATG</u>CGCGTTAACAATGGTT (*Nde* I site underlined) and <u>GAATTC</u>TTACAGTTTCG-GACCAGC (*Eco*R I site underlined). The mutated PCR-fragments (1.5 kb) were double-digested with *Nde* I and *Eco*R I, and then ligated with the same digested pET28a+ vector (Merck Millipore, Darmstadt, Germany). The vectors were transformed into the ER2566 strain and used for screening, enzyme purification, and characterization.

The selected PCK derivative (PCK67) was PCR-amplified from the template pET-Pck67, using the oligonucleotides <u>GAATTC</u>CGCGTTAACAATGGTT (*Eco*R I site underlined) and <u>CTGCAG</u>TTACAGTTTCGGACCAGC (*Pst* I site underlined). The DNA fragment was ligated with the same digested pTrc99a vector (GenBank M22744.1) after purification, resulting in pEcPck67, and further

Table 1 Strains and plasmids used in this study

Strains	Description	Source
W3110	*E. coli* K-12 wild-type	KCTC 2223
W3110 *ppc$^-$*	W3110 *ppc*5::*kan*, Km^R	[19]
W3110 P$_{ppc}^-$ *pckA*	W3110 with the promoter region (200 bp) of *pckA* gene is replaced with *ppc* promoter in chromosome	[21]
DH5α	F$^-$ Φ80*lacZ*ΔM15 Δ(*lacZYA-arg*F) U169 *rec*A1 *end*A1 *hsd*R17 (r$_K^-$, m$_K^+$) *pho*A *sup*E44 λ$^-$ *thi*-1 *gyr*A96 *rel*A1	Invitrogen
ER2566	*E. coli* F$^-$ *ompT gal dcm lon hsdSB* (r$_B$-m$_B$-; *E. coli* B strain), with DE3, a λ prophage carrying the T7 RNA pol gene	NEB
Plasmids		
pET28a(+)	Protein expression vector, T7 promoter, Km^R	Merck millipore
pTrc99a	Expression vector, *trc* promoter, Ap^R	GenBank M22744.1
pTrc-*hemA* + -*maeA*-*dctA*	pTrc99a containing *hemA*, *maeA*, and *dctA* genes. Template for dicarboxylate transporter (*dctA*) PCR-amplification.	[24]
pET-Pck	pET28a+ containing mutated *pckA* gene at *Nde* I-*Eco*R I with N-terminal 6-His tag.	This study
pEcPck	pTrc99a containing *E. coli* PCK$_{WT}$ gene at *Eco*R I-*Pst* I sites, Ap^R	[10]
pEcPck67	pTrc99a containing *E. coli*, the evolved PCK (PCK67) gene at *Eco*R I-*Pst* I sites, Ap^R	This study
pKJ606-GR	*Gloeobacter* rhodopsin *gll0198* gene at *Nde* I-*Hind* III sites, *lac* promoter, Ap^R	[23]
pKJ606-*dctA*	*E. coli* dicarboxylate transporter (dctA) gene at *Nde* I-*Not* I sites, *lac* promoter, Ap^R	This study

Km kanamycin, *Ap* ampicillin, ^{R} antibiotic resistance

transformed into the strain W3110. Oligonucleotide synthesis and DNA sequencing were carried out in the facility of Macrogen Co. (Seoul, Korea).

Culture conditions

All *E. coli* strains were grown in Luria–Bertani (LB) medium [34]. The W3110 derivatives expressing PCK were grown in LB glucose-based medium [13, 19]. A single colony was inoculated in 3 mL of LB medium containing ampicillin (50 µg/mL) and incubated at 37 °C and 220 rpm. Next, 500 µL of overnight grown culture was then transferred into a 250 mL Erlenmyer flask containing 50 mL of medium (25 g/L LB broth, 50 µg/mL ampicillin, 0.1 mM isopropyl *β*-D-thiogalactopyranoside (IPTG), 9 g/L glucose, 10 g/L sodium bicarbonate). A glutathione stock was dissolved in 0.1 mM dithiothreitol (DTT) solution to prevent oxidation, and added to the media at concentrations of 0–1 mM when necessary. Cells were incubated at 37 °C and 220 rpm for 8 h, and samples were taken every hour.

For the anaerobic cultures of the W3110 derivatives expressing PCK, a 150 mL anaerobic glass serum vial (Bellco Glass Inc., Vineland, NJ, USA) containing 100 mL of the LB glucose-based medium was tightly sealed with a rubber bung with an aluminum cap and further flushed repeatedly with nitrogen gas to remove oxygen prior to inoculation. One mL of overnight grown *E. coli* strains were inoculated to the sterilized anaerobic vials using a 1 mL syringe and the inoculated vial was maintained at 37 °C

and 100 rpm. Culture broth samples were taken using a 1 mL syringe to avoid oxygen contamination.

Batch cultures of the W3110 expressing membrane-integrated proteins were performed in LB glucose-based medium [34] under illumination or dark conditions [6, 22]. A single colony was cultured in a 15 mL tube containing 3 mL of LB medium with ampicillin (50 µg/mL) at 37 °C and 220 rpm overnight, and then an aliquot (500 µL) was transferred to a 250 mL Erlenmyer flask containing 50 mL of minimal media (3 g/L glucose, 0.1 mM IPTG, 50 µg/mL ampicillin, 0.8 g/L NH$_4$Cl, 0.5 g/L NaCl, 7.5 g/L Na$_2$HPO$_4$·2H$_2$O, 3 g/L KH$_4$PO$_4$, 0.2 g/L MgSO$_4$·7H$_2$O, 0.1 g/L CaCl$_2$, 1 mg/L thiamine·HCl) supplemented with all-trans-retinal (Sigma) (5 µM, dissolved in ethanol). For illumination conditions, the *E. coli* expressing GR were then cultured in a rotary shaking incubator (37 °C and 220 rpm) equipped with light bulb illumination (two 13 W bulbs at a 20-cm distance). For dark conditions, 250 mL Erlenmyer flasks were wrapped with aluminum foil and turned the light bulb off during the cultivation. Batch cultures of the W3110 expressing GR or DctA were performed in the dark conditions. Samples were taken every hour. All batch experiments were repeated at least 3 times.

Chemostat cultures of W3110 expressing PCK$_{WT}$ were performed in minimal glucose-based medium to determine the intracellular ATP and ROS concentrations at the steady states. One milliliter of overnight culture of a single colony, grown in LB medium containing ampicillin (50 µg/mL), was transferred to a 250 mL fermenter jar (Mini-Chemostat

Fermenter; Hanil Inc., Bucheon, Korea) containing 100 mL of M9 minimal glucose medium (3 g/L glucose, 0.1 mM IPTG, 50 µg/mL ampicillin, 0.8 g/L NH_4Cl, 0.5 g/L NaCl, 7.5 g/L $Na_2HPO_4 \cdot 2H_2O$, 3 g/L KH_4PO_4, 0.2 g/L $MgSO_4 \cdot 7H_2O$, 0.1 g/L $CaCl_2$, 1 mg/L thiamine·HCl). The fermenters were operated at 37 °C and 200 rpm with aeration (150 mL/min). The fresh feed medium (2 L) had the same composition as the initial medium. The inlet and outlet flow rates were set at 10, 20, and 30 mL/h (dilution rates of 0.1, 0.2, and 0.3 h^{-1}, respectively). Steady-state samples were taken after 10 turnovers of the culture volume.

Screening and characterization

The ER2566 strain carrying the pET28a+ vector with *pckA* derivatives was grown on LB agar plates containing kanamycin (50 µg/mL), and then the colonies were transferred to a 96-well plate containing 400 µL of LB-kanamycin medium. The cells were incubated overnight at 37 °C, 500 rpm, and then 40 µL was used to inoculate another 96-well plate containing 360 µL of fresh medium supplemented with IPTG (0.1 mM). The cells were allowed to express enzymes for 6 h at 37 °C, 500 rpm. After incubation, 200 µL of culture was mixed with 20 µL of lysis buffer (EasyLyse bacterial protein extraction buffer, Epicentre, Madison, WI, USA) and 4 µL of 1 M $MgCl_2$ to disrupt the cells for 10 min at room temperature. The lysed cell extract (50 µL) was then reacted with 150 µL of reaction buffer [2 mM PEP, 50 mM $NaHCO_3$, 5 mM $MgCl_2$, and 2 mM ADP in 100 mM HEPES (2-[4-(2-hydroxyethyl) piperazin-1-yl] ethanesulfonic acid) buffer, pH 7.0, 2.5 U of malate dehydrogenase, 0.14 mM NADH]. After a 10 min reaction at 37 °C, the OAA production was estimated by measuring the absorbance at 340 nm, with an extinction coefficient of 6.22 mM^{-1} cm^{-1}. Among the tested colonies, 3 displaying increased enzyme activities were selected and subjected to purification using Ni^{+}-affinity chromatography. Enzyme kinetic parameters were determined as previously described [21].

Analysis

Cell growth was measured by determining the optical density at 600 nm ($OD_{600 nm}$) and then converted into dry cell weight (DCW) using the coefficient of 0.31 g/L.

Intracellular ATP concentration was immediately determined after sampling using an ATP bioluminescent assay kit (Sigma-Aldrich, MO, USA) and a luminometer (Promega, Madison, WI, USA), according to the manufacturer's instructions. Measurement was performed after sampling and disrupting the cells by sonication (UP200S ultrasonic processor, Hielscher Ultrasonics Co., Teltow, Germany) at 140 W for 30 s on ice [12].

Relative ROSs of the cells were determined using CM-H_2DCFDA (5-[and -6]-chloromethyl-2′,7′ -dichlorodihydrofluorescein diacetate), a free radical indicator [37]. A 1 mL aliquot of steady-state cells was harvested from the chemostat (Biotron Inc., Bucheon, Korea), washed with 50 mM phosphate buffer (0.2 mL, pH 7.0), and mixed with 20 µM CM-H_2DCFDA (dissolved in dimethyl sulfoxide). After incubation for 30 min at 37 °C, the supernatant was discarded and the pellet was re-suspended in 0.2 mL of the same buffer, then subjected to disruption by sonication (140 W, 30 s) on ice. Cell extracts were transferred into a 96-well black-walled plate with a flat bottom, and the fluorescence intensity was measured using a fluorometer reader (Synergy MX, BioTek, VT, USA) with excitation/emission at 492/530 nm, respectively. Relative ROS was displayed as the ratio of $ROS_{sample}/ROS_{control}$. The ATP and ROS concentrations were analyzed at least 3 times.

Results

Directed evolution of PCK

To acquire a PEP carboxykinase (PCK) with greater enzymatic activity, random mutations were introduced into the wild-type PCK gene (*pckA*). Among 600 clones expressing mutated enzymes, three were selected based on the greater enzyme activity displayed than the original cell extracts. The enzyme activities of the selected clones were characterized after purification (Table 2). The clone PCK67 demonstrated the greatest increase of PEP carboxylation activity, with 62 % greater catalytic efficiency for the PEP substrate than that of PCK_{WT}, with the same catalytic efficiency for the bicarbonate substrate. The DNA sequencing results of PCK67 indicated that 748 T was changed to G, resulting in change of the serine residue at 250 to alanine.

Effect of PCK-overexpression-mediated increase of ATP on growth rate

To investigate the relationship between artificial ATP increase and growth rate, the activities of ATP-generating enzymes were determined by examining the growth rates of cells expressing the PCK_{WT} or the evolved PCK (PCK67) in different host backgrounds (Table 3). Wild-type *E. coli* carrying empty vector, which should have the lowest intracellular PCK activity among the tested strains, showed a maximum growth rate of 1.03 h^{-1} and the intracellular ATP concentration of 0.28 µmol/g_{cell} at log phase under the given conditions. The W3110 P_{ppc}^{-} *pckA* strain expressed the *pckA* gene under the control of the glycolytic

Table 2 Characteristics of PEP carboxykinase derivatives

Strains	For PEP substrate			For HCO_3^{-1} substrate		
	K_m (mM)	k_{cat} (min^{-1})	Catalytic efficiency (k_{cat}/K_m)	K_m (mM)	k_{cat} (min^{-1})	Catalytic efficiency (k_{cat}/K_m)
PCK$_{WT}$	0.18 ± 0.01	7.6 ± 2.1	41.7 ± 14.0	31.7 ± 10.1	17.4 ± 3.2	0.56 ± 0.08
PCK67	0.10 ± 0.06	6.5 ± 2.3	67.8 ± 14.3	34.1 ± 9.7	18.6 ± 0.8	0.56 ± 0.14
PCK404	0.16 ± 0.03	7.1 ± 0.4	46.5 ± 11.5	69.5 ± 4.1	31.5 ± 2.5	0.46 ± 0.06
PCK506	0.13 ± 0.01	6.1 ± 1.3	45.1 ± 11.3	37.1 ± 3.4	18.6 ± 2.8	0.50 ± 0.03

Data are represented as mean ± SD from at least three independent experiments

Table 3 Effects of PCK-derived artificial ATP increase on growth rate under aerobic conditions

Strains	Specific growth rate (h^{-1})	Intracellular ATP (μmol/g$_{cell}$)[a]	Relative ROS (relative fold, from the repeated experimental set)[b]	Description
W3110 (pTrc99a)	1.03 ± 0.067	0.28 ± 0.023	1.00	Control. Wild-type *E. coli* carrying empty vector
W3110 P$_{ppc}^-$ pckA (pTrc99a)	0.86 ± 0.008	0.54 ± 0.051	1.34 ± 0.19	*pckA* gene expression under control of *ppc* promoter in genome, [21]
W3110 (pEcPck)	0.84 ± 0.040	1.00 ± 0.052	1.13 ± 0.41	Wild-type *E. coli* over-expressing *pckA* from plasmid
W3110 (pEcPck67)	0.66 ± 0.057	1.45 ± 0.065	1.60 ± 0.15	Wild-type *E. coli* overexpressing PCK67 from plasmid

Data from W3110 *ppc*⁻ host background were not displayed because the strains were not grown enough at the given conditions

ND not determined

[a] ATP concentrations were determined at mid-log phase (4 h). Data are represented as mean ± SD from at least three independent experiments

[b] Data from the repeated experimental sets to measure ROS concentrations

ppc promoter from its chromosome, and previous study had shown ~80 % of the PEP carboxylation reaction was a result of PPC while ~20 % PCK [21]. This promoter engineered strain was expected to have higher PCK activity than the wild-type strain, and showed a slower growth rate with more accumulation of ATP (0.86 h^{-1} and 0.54 μmol/g$_{cell}$, respectively). The *E. coli* overexpressing PCK from the plasmid, expected to display the highest PCK$_{WT}$ activity, showed an even lower growth rate of 0.84 h^{-1}, with the ATP concentration of 1.00 μmol/g$_{cell}$. Upon overexpression of PCK67, which possessed 60 % greater activity than PCK$_{WT}$, the highest overall ATP concentration of 1.45 μmol/g$_{cell}$ and lowest growth rate of 0.66 h^{-1} were observed.

PPC (PEP carboxylase) shares substrates (PEP and bicarbonate) with PCK (PEP carboxykinase). To eliminate competition for substrate, the wild-type strain was replaced with a PPC-disrupted strain (W3110 *ppc*⁻). The W3110 *ppc*⁻ derivatives could hardly grow in glucose-containing media (both a minimal glucose and a LB glucose medium), though the strains grew well in complex medium (LB)

without glucose presence, and the intracellular ATP concentration could not be determined.

Relationship between PCK-mediated artificial ATP increase and ROS

Because toxic reactive oxygen species (ROS) are generated within the electron transfer chain in energy metabolism, which is related to membrane potential, it was assumed that the artificial increase of ATP might also have accelerated the diversion of electrons to oxygen molecules, resulting in an increase of the ROS. To verify this assumption, chemostat cultures were performed, and the intracellular ATP and ROS concentrations were estimated using steady-state cells (Fig. 1). The intracellular ATP concentration itself was not directly related to the growth rate; however, the difference in ATP between the control (W3110 [empty vector]) and the strain overexpressing PCK$_{WT}$ (W3110 [pEcPck]) increased as the dilution rate increased (ΔATP = 0.3 μmol/g$_{cell}$, ΔATP = 0.45 μmol/g$_{cell}$, ΔATP = 1.05 μmol/g$_{cell}$ at 0.1, 0.2, and 0.3 h^{-1}, respectively). At the same time, while
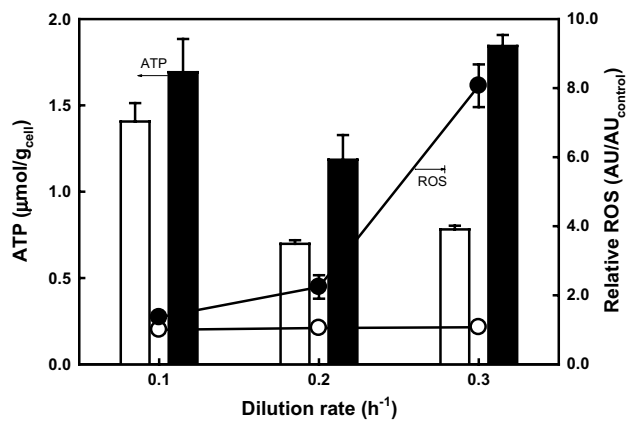
Fig. 1 Intracellular ATP and relative ROS contents of PCK-overexpressing *E. coli* at steady state. *Bars* represent for ATP and symbols for ROS Control, W3110 strain carrying empty vector (*white circle*, *white bar*); PCK$_{WT}$, W3110 strain carrying pEcPck (*black circle*, *black bar*). Data are represented as mean ± SD from at least three independent experiments

Table 4 Effects of glutathione addition on growth retardation caused by PCK-derived artificial ATP increase

Strain	Glutathione concentration (mM)	Growth rate (h^{-1}, log phase)
W3110 (empty vector)	0	0.98 ± 0.074
	0.1	0.95 ± 0.060
	1	0.97 ± 0.068
W3110 (pEcPck)	0	0.79 ± 0.075
	0.1	0.96 ± 0.066
	1	1.00 ± 0.044

Data are represented as mean ± SD from at least three independent experiments

great variation of the ROS concentrations did not occur in the control, the PCK$_{WT}$-overexpressing W3110 showed drastic increase of the ROS as the ΔATP increased. The ROS differences between the control and the PCK$_{WT}$-overexpressing strain were as follows: ΔROS = 0.5 AU (arbitrary unit)/g$_{cell}$ at $D = 0.1$ h^{-1}, ΔROS = 1.2 AU/g$_{cell}$ at $D = 0.2$ h^{-1}, and ΔROS = 7.2 AU/g$_{cell}$ at $D = 0.3$ h^{-1}. The W3110 (pEcPck) never reached the steady state at $D = 0.4$ h^{-1} or higher dilution because it was eventually washed out, though the control strain could grow at $D = 0.4$ h^{-1} or higher dilution rate. Therefore, the artificial ATP increase was correlated to the ROS concentration in steady-state cells.

To verify this chemostat results, batch cultures of the few PCK-derived artificial ATP-increased strains from the previous results were repeated and their ROS concentrations were analyzed (Table 3, repeated experimental set). Indeed, the strains with the artificial ATP increase by *pckA* promoter exchange and Pck67-overexpression (W3110 P$^-_{ppc}$*pckA* [pTrc99a] and W3110 [pEcPck67] in Table 3) contained 34 and 60 % greater intracellular ROS than the control, respectively. Therefore, it was confirmed that the PCK-derived artificial ATP-increased strains contained greater ROS concentration in chemostat and batch cultures.

Effect of ROS scavenger on growth rate in PCK-overexpressing *E. coli*

To confirm that the observed increase in ROS caused by the artificial ATP increase was related to the growth retardation, cells were grown in medium containing glutathione as an antioxidant, and their growth rates in the log phase

were estimated (Table 4). The growth rate of the control strain (W3110 harboring an empty vector) did not vary depending on the glutathione concentration, which was added in the range of 0–1 mM. However, the strain with artificial ATP increase (W3110 [pEcPck]) demonstrated recovery of the growth rate as the glutathione concentration increased. The growth retardation of W3110 (pEcPck) was fully recovered in the 0.1 mM glutathione-containing medium.

Effect of ATP increase via expression of bacteriorhodopsin on growth rate

Because the overexpression of PCK or knockout of PPC might have caused perturbations of metabolic flux (between PEP and OAA node), the PCK-derived artificial ATP increase might have not been directly related to the growth retardation. To clear the issue by eliminating the perturbation of carbon flux, *Gloeobacter* rhodopsin (GR), a light-induced proton pump [6, 23], was introduced into *E. coli*, and the cells were cultured under illumination (Fig. 2a). *Escherichia coli* W3110 (empty vector), the negative control, displayed the maximum growth rate of 0.35 h^{-1}, with the intracellular ATP concentration of 0.72 μmol/g$_{cell}$ and ROS of 905 AU/g$_{cell}$ at the log phase. In contrast, the W3110 (pKJ606-GR) strain displayed the lower growth rate of 0.19 h^{-1}, the higher intracellular ATP of 1.14 μmol/g$_{cell}$ and ROS of 1646 AU/g$_{cell}$ which corresponded to a 47 % lower growth rate with 81 % greater intracellular ATP and 82 % greater relative ROS than the control. The artificial ATP increase without carbon flux variation (GR-expression+illumination) also reduced growth rate with increase of ROS.

In the dark conditions (no artificial ATP increase conditions), growth profiles of *E. coli* strains expressing GR and dicarboxylate transporter (*dctA*), a control membrane-integrated protein with no energy generation, were also examined (Fig. 2b, c). The GR-expression under dark conditions
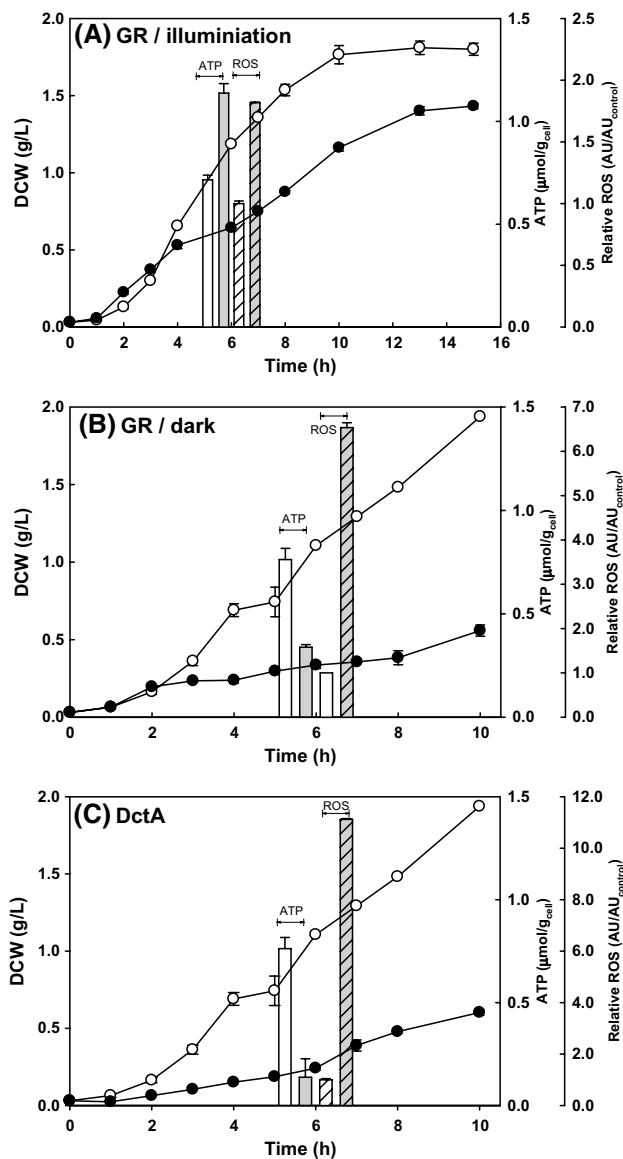
Fig. 2 Growth profile, intracellular ATP, and ROS of membrane-integrated protein expressing *E. coli* strains. **a** GR-expression under illumination, **b** GR-expression under dark conditions, **c** DctA-expression. *Circle symbols* for growth, *open bars* for ATP, and *shaded bars* for ROS Control, W3110 strain carrying empty vector (*white circle*, *white bars*); membrane protein expressions (*black circle*, *gray bars*). ATP and ROS were measured at 6 h. Data are represented as mean ± SD from at least three independent experiments

even reduced the growth rate (26 % of control) with elaborated ROS (6.5-fold of control). The ATP concentration was 0.34 $\mu mol/g_{cell}$ (vs. 0.76 $\mu mol/g_{cell}$ of control). The DctA-expressing *E. coli* also showed similar trend with the GR-expressing *E. coli* under dark conditions, reduced growth rate (61 % of control), elaborated ROS (11.1-fold of control), with lower ATP level (0.14 $\mu mol/g_{cell}$ vs. 0.76 $\mu mol/g_{cell}$ of control).
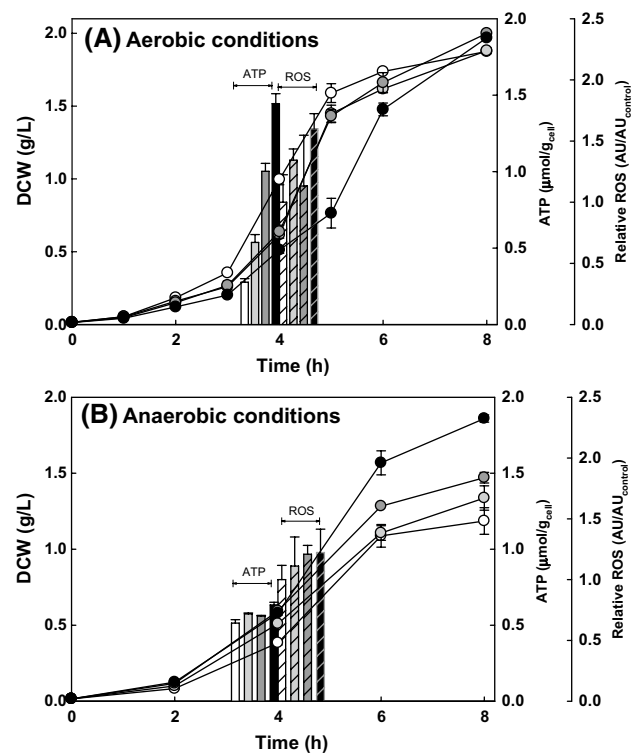

Fig. 3 Growth profiles, intracellular ATP, and ROS of PCK-derived artificial ATP-increased *E. coli* strains. **a** Aerobic conditions, **b** Anaerobic conditions. *Circle symbols* for growth, *open bars* for ATP, and *shaded bars* for ROS Control, W3110 carrying empty vector (*white*); W3110 P^-_{ppc} *pckA* (*light gray*); W3110 overexpressing PCK$_{WT}$ (*dark gray*); W3110 overexpressing PCK67, (*black*). ATP and ROS were measured at mid-log phase (4 h for aerobic conditions). Data are represented as mean ± SD from at least three independent experiments

Growth rate comparison of the PCK-mediated artificial ATP increases under anaerobic conditions

All the evidences of the above agreed that the ROS increase came from the artificial ATP increase was the reason of the growth retardation. To complement the theory, *E. coli* strains with various artificial ATP increase levels were cultivated under strict anaerobic conditions, which no ROS should be provoked, and compared with the growth under aerobic conditions (Fig. 3). Under aerobic conditions, the most ATP-harboring strain (W3110 [pEcPck67]) had the most ROS and the slowest growth rate (Fig. 3a, came from the data set of Table 3). Unlike the aerobically grown *E. coli* strains that showed the reciprocal relationship between the growth rate and the artificial ATP increase, no oxygen conditions enabled the *E. coli* strains to grow faster as the more artificial ATP increased in order of W3110(pEcPck67) > W3110(pEcPck) > W3110 P^-_{ppc} *pckA*(empty vector) > W3110(empty vector) (Fig. 3b). Relative ROS was varied in a limited range of ~1.2-fold compared with those from the aerobic conditions (relative ROS ~1.8-fold).

Discussion and conclusions

Artificial ATP increases of cells could have biotechnological benefits, such as allowing enhancement of the translation and secretion of recombinant protein [12]. Active transport of fermentation substrate influx and product efflux could be another potential benefit of using cells harboring extra ATP considering that the energy state in *E. coli* (logarithm function of [ATP]/[ADP]) was linearly correlated to the activity of phosphotransferase uptake system [32], and one might expect that artificial ATP increase would enhance the glucose-derived metabolism. However, observed retardation of the growth rate caused by the artificial increase of ATP was noted as a limitation for bio-process applications [21]. The results of this study indicated that the artificial increase in ATP indeed caused the cells to grow more slowly, in a dose-dependent manner (Tables 3; Fig. 1). The artificial ATP increase was achieved herein by the "extra ATP-generating" activities of PCK, and the growth rate was observed to be inversely related to the amount of ATP (Table 2; Fig. 3a). The strain overexpressing the PCK mutant with the highest activity (PCK67) without a substrate-competing PEP carboxylase (PPC) host (W3110 *ppc⁻*), expected to harbor the greatest ATP concentration, did not grow in the presence of glucose as other reports (no growth under aerobic conditions of *ppc*-disrupted *E. coli* on M9 medium with glucose [31], on M9 medium with glycerol [10], and MOPS medium with glucose [1]). The results from expression of *Gloeobacter* rhodopsin (GR) also agreed with the theory that growth was inhibited by the artificial ATP increase (Fig. 2a). The artificial ATP increase by GR-expression contributed to the increase of ATP under illumination conditions, resulting in

reduction of the growth rate. Because the ATP increases by GR-expression did not provoke perturbations of the carbon flux, unlike those by metabolic PCK expression, this result confirmed that the artificial ATP increase itself was responsible for the observed growth retardation.

Superoxide radical, hydroxyl radical, and hydrogen peroxide are reactive oxygen species (ROS), which are mainly formed during respiration by the incomplete reduction of oxygen [8]. Because oxidative stress caused by the high oxidizing potential of ROS leads to cellular damage, such as mutations and metabolic pathway disruption, increases of ROS could inhibit cell growth [22]. ROS damage from the oxygenic bio-process of aerobic organisms is unavoidable, so cells defend themselves by expressing ROS-neutralizing enzymes, or by producing ROS-scavenging metabolites [28]. We suspected that ATP synthase and the electron transfer reactions might somehow be influenced by the artificial increase of ATP, and that oxygen, the final electron acceptor, might consequently be incompletely reduced. Indeed, the *E. coli* with artificial ATP increase showed a dramatic increase of ROS at the steady state (Fig. 1) and the repeated experimental sets of batch cultures (Table 3). Conversely, the addition of the antioxidant glutathione (>0.1 mM) into the media allowed restoration of the retarded growth of the *E. coli* (Table 4) (The intracellular glutathione concentration in glucose-fed, exponentially growing *E. coli* was known to be 2.4 mM [2]), which supports the theory that retardation of the growth rate by artificial ATP increase was mediated by increased ROS. In the no ROS-provoking (strict anaerobic) conditions, the growth of artificial ATP-increased strains even grew faster than control strain (Fig. 3b). In the case of eukaryotic mitochondrial oxidation state, it was reported that the correlations

Table 5 Variation of transcriptome of high ATP-charged cells, focused on defense against ROS

Gene name[a]	Gene description[b]	ID[c]	log₂(cy5/cy3)[d]	Fold change
sodB	Superoxide dismutase, Fe–Mn family, [EC:1.15.1.1]	CC1391	−0.7884	0.58
sodC	Superoxide dismutase, Cu–Zn family, [EC:1.15.1.1]	CC1381	−0.7280	0.60
grxC	Glutaredoxin 3	CC3015	−0.5799	0.67
ahpF	Alkyl hydroperoxide reductase, F52a subunit, [EC:1.6.4.-]	CC0500	−0.3004	0.81
trxA	Thioredoxin 1	CC3164	−0.0014	0.99
tpx	Lipid hydroperoxide peroxidase, [EC:1.11.1.15]	CC1137	0.02715	1.02
ahpC	Alkyl hydroperoxide reductase, C22 subunit, [EC:1.11.1.15]	CC3819	0.1150	1.08
katE	Catalase/hydroperoxidase HPII(III), [EC:1.11.1.6]	CC1465	0.2066	1.15
gor	Glutathione oxidoreductase, [EC:1.8.1.7]	CC2913	0.2714	1.21
katG	Catalase/hydroperoxidase HPI(I), [EC:1.11.1.21]	CC3302	0.2821	1.22
sodA	Superoxide dismutase, Fe–Mn family [EC:1.15.1.1]	CC3270	0.3185	1.25
gshA	γ-Glutamate-cysteine ligase (glutathione synthetase), [EC:6.3.2.2]	CC2195	0.4594	1.37

[a,b] Information was obtained from NCBI and KEGG (http://www.ncbi.nlm.nih.gov; http://www.kegg.jp)

[c,d] Transcriptome data were adapted from GEO microarray results (http://www.ncbi.nlm.nih.gov/geo; access code: GSM211801) of the previous publication [20]

between ATP and ROS can result in programmed cell death and axonal degeneration [29, 33]. Similar studies in other species were found to support the hypothesis that the growth retardation by ROS can be recovered by the use of antioxidants as free radical scavengers in other living organisms [25, 35].

Mechanistic reason of the ROS increase by the artificial ATP increase requires more studies. A plausible explanation is that the artificial-driven ATP increase might have led more protons accumulation across membrane and the strengthened membrane potential might further have influenced on many membrane-bound dehydrogenases and mobile electron carriers to mis-transfer a pair of electrons to oxygen molecule, which would increase ROS. Although an *E. coli* expressing periplasmic recombinant protein (e,g., human interleukin-2) has been reported to provoke ROS increase [26], the growth defect therefrom was not as severe as the expression of membrane-integrated proteins in this study (Fig. 2b, c). The overexpression of membrane-integrated proteins, i.e., GR under dark conditions and dicarboxylate transporter, should have interfered the movement of electron carriers, ed the drastic ROS increase (6.5-fold Fig. 2b and 11.1-fold in Fig. 2c). These results would strengthen the plausible explanation. Measuring the redox state of membrane components, genetic deletions of the proteins in oxidative phosphorylation [3] would be also helpful to understand the mechanistic reason.

Although *E. coli* possesses many genes to defend against ROS, it might have incorrectly responded to the additional ROS driven by the artificial increase in ATP, an unnatural physiological condition. Table 5 presents the variation of ROS defense genes in the PCK-overexpressing *E. coli* W3110 at $D = 0.1$ h^{-1} steady state in complex glucose medium [20]. The previous DNA microarray results indicated that the higher ATP-harboring cell by the PCK-overexpression up-regulated the transcriptions of genes in biosynthetic pathway (i.e., amino acids and nucleotides) and flagella structural genes, while down-regulated the transcription of genes in carbon metabolism (Gene Expression Omnibus access code: GSM211801). Superoxide dismutases, peroxidases, and catalases, however, were slightly down-regulated or showed no difference in expression levels even though the ATP was artificially increased, which must have increased the ROS levels as well. If the ROS defense genes have been expressed in the strain with artificial ATP increase, one might expect recovery of the growth rate without the addition of antioxidants to the medium. The artificial ATP increase was correlated with the faster growth rate and yield under the anaerobic conditions (Fig. 3), which support the above expectation.

In conclusion, the reduction in growth rate occurred as a result of the artificial ATP increase, coupled with increase in intracellular ROS, regardless of carbon perturbation. The growth rate could be even faster as the more artificial ATP increase under anaerobic conditions. Therefore, an ROS removal strategy is required for metabolically engineered cells harboring greater ATP for practical applications.

References

1. Baba T, Ara T, Hasegawa M, Takai Y, Okumura Y, Baba M, Datsenko KA, Tomita M, Wanner BL, Mori H (2006) Construction of *Escherichia coli* K-12 in-frame, single-gene knockout mutants: the Keio collection. Mol Syst Biol 2(2006):0008. doi:10.1038/msb4100050

2. Bennett BD, Kimball EH, Gao M, Osterhout R, Van Dien SJ, Rabinowitz JD (2009) Absolute metabolite concentrations and implied enzyme active site occupancy in *Escherichia coli*. Nat Chem Biol 5:593–599. doi:10.1038/nchembio.186

3. Causey TB, Zhou S, Shanmugam KT, Ingram LO (2003) Engineering the metabolism of *Escherichia coli* W3110 for the conversion of sugar to redox-neutral and oxidized products: homoacetate production. Proc Natl Acad Sci USA 100:825–832. doi:10.1073/pnas.0337684100

4. Chao YP, Liao JC (1993) Alteration of growth yield by overexpression of phosphoenolpyruvate carboxylase and phosphoenolpyruvate carboxykinase in *Escherichia coli*. Appl Environ Microbiol 59:4261–4265

5. Chao YP, Liao JC (1994) Metabolic responses to substrate futile cycling in *Escherichia coli*. J Biol Chem 269:5122–5126

6. Choi AR, Shi L, Brown LS, Jung K-H (2014) Cyanobacterial light-driven proton pump, *Gloeobacter* rhodopsin: complementarity between rhodopsin-based energy production and photosynthesis. PLoS ONE 9:e110643. doi:10.1371/journal.pone.0110643

7. Coomes MW, Mitchell BK, Beezley A, Smith TE (1985) Properties of an *Escherichia coli* mutant deficient in phosphoenolpyruvate carboxylase catalytic activity. J Bacteriol 164:646–652

8. Fridovich I (1998) Oxygen toxicity: a radical explanation. J Exp Biol 201:1203–1209

9. Izui K, Matsuda Y, Kameshita I, Katsuki H, Woods AE (1983) Phosphoenolpyruvate carboxylase of *Escherichia coli*. Inhibition by various analogs and homologs of phosphoenolpyruvate. J Biochem 94:1789–1795

10. Joyce AR, Reed JL, White A, Edwards R, Osterman A, Baba T, Mori H, Lesely SA, Palsson BO, Agarwalla S (2006) Experimental and computational assessment of conditionally essential genes in *Escherichia coli*. J Bacteriol 188:8259–8271. doi:10.1128/JB.00740-06

11. Kim HJ, Kang SY, Choi JH, Kim P (2012) Activity improvement of UDP-galactose-4-epimerase for tagatose substrates by 3D structure-based combinatorial mutagenesis. J Mol Catal B Enzym 84:35–39. doi:10.1016/j.molcatb.2012.04.020

12. Kim HJ, Kwon YD, Lee SY, Kim P (2012) An engineered *Escherichia coli* having a high intracellular level of ATP and enhanced recombinant protein production. Appl Microbiol Biotechnol 94:1079–1086. doi:10.1007/s00253-011-3779-0

13. Kim P, Laivenieks M, Vieille C, Zeikus JG (2004) Effect of overexpression of *Actinobacillus succinogenes* phosphoenolpyruvate carboxykinase on succinate production in *Escherichia*

coli. Appl Environ Microbiol 70:1238–1241. doi:10.1128/aem.70.2.1238-1241.2004

14. Kim S, Lee CH, Nam SW, Kim P (2011) Alteration of reducing powers in an isogenic phosphoglucose isomerase (*pgi*)-disrupted *Escherichia coli* expressing NAD(P)-dependent malic enzymes and NADP-dependent glyceraldehyde 3-phosphate dehydrogenase. Lett Appl Microbiol 52:433–440. doi:10.1111/j.1472-765X.2011.03013.x

15. Kim S, Moon DB, Lee CH, Nam SW, Kim P (2009) Comparison of the effects of NADH- and NADPH-perturbation stresses on the growth of *Escherichia coli*. Curr Microbiol 58:159–163. doi:10.1007/s00284-008-9294-6

16. Krebs A, Bridger WA (1980) The kinetic properties of phosphoenolpyruvate carboxykinase of *Escherichia coli*. Can J Biochem 58:309–318. doi:10.1139/o80-041

17. Krupinski J, Hammes GG (1986) Steady-state ATP synthesis by bacteriorhodopsin and chloroplast coupling factor co-reconstituted into asolectin vesicles. Proc Natl Acad Sci USA 83:4233–4237

18. Kwon YD, Kwon OH, Lee HS, Kim P (2007) The effect of NADP-dependent malic enzyme expression and anaerobic C4 metabolism in *Escherichia coli* compared with other anaplerotic enzymes. J Appl Microbiol 103:2340–2345. doi:10.1111/j.1365-2672.2007.03485.x

19. Kwon YD, Lee SY, Kim P (2006) Influence of gluconeogenic phosphoenolpyruvate carboxykinase (PCK) expression on succinic acid fermentation in *Escherichia coli* under high bicarbonate condition. J Microbiol Biotechnol 16:1448–1452

20. Kwon YD, Lee SY, Kim P (2008) A physiology study of *Escherichia coli* overexpressing phosphoenolpyruvate carboxykinase. Biosci Biotechnol Biochem 72:1138–1141. doi:10.1271/bbb.70831

21. Lee HJ, Kim HJ, Seo J, Na YA, Lee J, Lee JY, Kim P (2013) Estimation of phosphoenolpyruvate carboxylation mediated by phosphoenolpyruvate carboxykinase (PCK) in engineered *Escherichia coli* having high ATP. Enzyme Microbial Technol 53:13–17. doi:10.1016/j.enzmictec.2013.04.001

22. Lee JY, Lee HJ, Seo J, Kim ES, Lee HS, Kim P (2014) Artificial oxidative stress-tolerant *Corynebacterium glutamicum*. AMB Express 4:15. doi:10.1186/s13568-014-0015-1

23. Lee KA, Jung K-H (2011) ATP regeneration system using *E. coli* ATP synthase and *Gloeobacter* rhodopsin and its stability. J Nanosci Nanotechnol 11:4261–4264. doi:10.1166/jnn.2011.3669

24. Lee MJ, Kim HJ, Lee JY, Kwon AS, Jun SY, Kang SH, Kim P (2013) Effect of gene amplifications in porphyrin pathway on heme biosynthesis in a recombinant *Escherichia coli*. J Microbiol Biotechnol 23:668–673

25. Lin J-N, Kao CH (1998) Effect of oxidative stress caused by hydrogen peroxide on senescence of rice leaves. Bot Bull Acad Sinica 39:161–165

26. Mahmoudi Azar L, Mehdizadeh Aghdam E, Karimi F, Haghshenas B, Barzegari A, Yaghmaei P, Hejazi MS (2013) Influence of foreign DNA introduction and periplasmic expression of recombinant human Interleukin-2 on hydrogen peroxide quantity and catalase activity in *Escherichia coli*. Adv Pharm Bull 3:395–402. doi:10.5681/apb.2013.063

27. Miranda MR, Choi AR, Shi L, Bezerra AG Jr, Jung KH, Brown LS (2009) The photocycle and proton translocation pathway in a cyanobacterial ion-pumping rhodopsin. Biophys J 96:1471–1481. doi:10.1016/j.bpj.2008.11.026

28. Misra HS, Khairnar NP, Barik A, Indira Priyadarsini K, Mohan H, Apte SK (2004) Pyrroloquinoline-quinone: a reactive oxygen species scavenger in bacteria. FEBS Lett 578:26–30. doi:10.1016/j.febslet.2004.10.061

29. O'Donnell KC, Vargas ME, Sagasti A (2013) WldS and PGC-1alpha regulate mitochondrial transport and oxidation state after axonal injury. J Neurosci Off J Soc Neurosci 33:14778–14790. doi:10.1523/JNEUROSCI.1331-13.2013

30. Oh DK, Oh HJ, Kim HJ, Cheon J, Kim P (2006) Modification of optimal pH in L-arabinose isomerase from *Geobacillus stearothermophilus* for D-galactose isomerization. J Mol Catal B Enzym 43:108–112. doi:10.1016/j.molcatb.2006.06.015

31. Patrick WM, Quandt EM, Swartzlander DB, Matsumura I (2007) Multicopy suppression underpins metabolic evolvability. Mol Biol Evol 24:2716–2722. doi:10.1093/molbev/msm204

32. Rohwer JM, Jensen PR, Shinohara Y, Postma PW, Westerhoff HV (1996) Changes in the cellular energy state affect the activity of the bacterial phosphotransferase system. Eur J Biochem 235:225–230

33. Roy A, Ganguly A, BoseDasgupta S, Das BB, Pal C, Jaisankar P, Majumder HK (2008) Mitochondria-dependent reactive oxygen species-mediated programmed cell death induced by 3,3′-diindolylmethane through inhibition of F0F1-ATP synthase in unicellular protozoan parasite *Leishmania donovani*. Mol Pharmacol 74:1292–1307. doi:10.1124/mol.108.050161

34. Sambrook J, Russell DW (2001) Molecular cloning: a laboratory manual, 3rd edn. Cold Spring Harbor Laboratory Press, Cold Spring Harbor

35. Upadhyaya H, Khan MH, Panda SK (2007) Hydrogen peroxide induces oxidative stress in detached leaves of *Oryza sativa* L. Gen Appl Plant Physiol 33:83–95

36. Yang C, Hua Q, Baba T, Mori H, Shimizu K (2003) Analysis of *Escherichia coli* anaplerotic metabolism and its regulation mechanisms from the metabolic responses to altered dilution rates and phosphoenolpyruvate carboxykinase knockout. Biotechnol Bioeng 84:129–144. doi:10.1002/bit.10692

37. Yu T, Robotham JL, Yoon Y (2006) Increased production of reactive oxygen species in hyperglycemic conditions requires dynamic change of mitochondrial morphology. Proc Nat Acad Sci USA 103:2653–2658. doi:10.1073/pnas.0511154103